Soft Matter

PAPER

Cite this: *Soft Matter*, 2018, **14**, 1130

Chain conformation of poly(acrylic acid)-*graft*-poly(ethylene oxide)-*graft*-dodecyl in solution: an anomalous counter-ions condensation

Xinlu Zhou and Kongshuang Zhao *

Received 26th September 2017,
Accepted 2nd January 2018

DOI: 10.1039/c7sm01931a

rsc.li/soft-matter-journal

A dielectric spectroscopy study on a polyelectrolyte in aqueous solutions, which contains hydrophobic groups in part of the side chains poly(acrylic acid)-*graft*-poly(ethylene oxide)-*graft*-dodecyl (PAA-*g*-PEO-*g*-dodecyl) is reported. A refined double layer polarization model was proposed to analyze the double dielectric relaxations in the dielectric spectra. Various electrical and structural parameters of the copolymers were obtained. Besides the crossover concentration, another turning point around 4 mg mL^{-1} was identified through the analysis of all the dielectrical parameters including dielectric increment, relaxation time and correlation length. According to the scaling relationship between the correlation length and concentration, a necklace-like structure was predicted. In addition, 4 mg mL^{-1} was proven to be the transition point between string-controlling with bead-controlling structure of the chains. In addition, the fraction of effective charges on the chains was illustrated by Ito's counter-ions fluctuation theory, as well as its linear dependence relationship with the zeta potential. Meanwhile, the counter-ions condensation behavior was consistent with the avalanche-like trend, which was predicted by theory for a hydrophobic polyelectrolyte with a necklace conformation. The results demonstrated that the electrostatic interactions were the main driving force of the necklace-like structure with pendant globules when the string-controlling structure was below 4 mg mL^{-1}. While hydrophobic interactions are the main driving force of the structure of bead-controlling above 4 mg mL^{-1}.

1. Introduction

Polyelectrolytes (PEs) with some hydrophobic units in all or part of their backbone or side chains have attracted unquenchable attention over the past few decades due to their dual characteristics of aggregation ability and charged nature.[1] They have wide applications in the field of drug carriers,[2] tissue engineering,[3] self-assembly materials[4] and chemical industry.[5,6] Meanwhile, the competition of long-range electrostatic interactions with the short-range hydrophobic interactions and the presence of counter-ions make it very difficult to reach a similar level of understanding with their neutral or totally hydrophilic counterparts. Therefore, a comprehensive study on the role of various interactions and the effect of counter-ions on the chain conformation and solution properties is critically important.

Until now, the conformation of PE chains is still one of the important topics in the area of polymer physics and soft matter. A breakthrough stemmed from the scaling model proposed by de Gennes and Pfeuty *et al.*[7] In their work, the concept of correlation length ξ was defined to describe the conformation of hydrophilic PEs. In addition, a scaling relationship between the correlation length ξ and concentration was derived. Later, Dobrynin and Rubinstein *et al.*[8–10] introduced the scaling model into hydrophobic PEs. In their models, the chains were considered as a series of compact beads connected by narrow elongated strings. Within a finite polymer concentration, some counter-ions will condense on the chains due to the electrostatic attraction force from the charged monomers. For hydrophilic PEs, the fraction of effective charges decreases logarithmically upon increasing the polymer concentration. In a very dilute polymer solution, almost all the dissociated counter-ions leave the chains because of the high entropic penalty for counter-ions condensation.[11,12] There was a different mechanism for PEs in poor solution due to the hydrophobic micro-domains. An avalanche-like counter-ions condensation for hydrophobic PE with pearls necklace conformation was proposed by Andrey V. Dobrynin *et al.* Considering the counter-ions condensation, the chain dimensions of a hydrophobic PE solution with varying polymer or salt concentrations, solvent quality and fixed charge density were determined experimentally and using simulations.[13–17] However, the evolution of the chain conformation in the process of counter-ions condensation is still not well understood. A refined and accurate

College of Chemistry, Beijing Normal University, Beijing 100875, China. E-mail: zhaoks@bnu.edu.cn; Tel: +86-010-58805856

model used to describe the micro-structure of the chains in solution is still missing. In addition, an experimental analysis used to correlate the theoretical descriptions with the chains conformation and counter-ions condensation is also desirable.

Over the past two decades, numerous attempts have been made to explore various PE containing hydrophobic/hydrophilic side chains.[18–20] It was discovered that these copolymers easily form intermolecular aggregation or polymeric micelles in water at low concentrations. Such phenomena have widely been used in industrial and biomedical fields.[21–24] From a fundamental viewpoint, numerous works have still focused on the conformation transition of grafted PEs with different distribution of hydrophobic blocks[25] and degree of dissociation[26] of polyelectrolyte blocks, as well as the solution conditions[27] over the diluted solution. Nevertheless, the phenomenon of counter-ions condensation has often been ignored in this previous research and the concentration regimes are limited to dilute solutions. Several important questions need to be addressed and are worthy of further exploration, including how collapsing chains collect counter-ions, how the condensation affects their conformation, how the competition between the electrostatic and hydrophobic interactions affect the conformation transition of PEs.

The conformation and electrical properties on the chains of PEs have been studied using various techniques including scattering spectroscopy,[16] micro-rheology technology,[28,29] conductometry and osmotic measurements.[30] However, what is "happening" next to the PE or the interactions in the vicinity of the chains.[31] To further understand the conformation of PEs in solution over a wide concentration range, dielectric relaxation spectroscopy (DRS) was applied to study the conformation of a grafted PE. Due to its sensibility to the fluctuation of dipoles over an extraordinary wide frequency range from Hz to GHz, DRS was successfully applied to obtain various information including the local and total conformation,[32] effective charges,[33] the state of the counter-ions around the chains,[31,34] as well as the complex interactions.[35] Previously, Mandel's work[36] derived an empirical relationship between the dielectric increment and concentration based on the assumption that a flexible chain was a sequence of charged rod-like subunits. On the basis of a cell model and the assumption that the fraction of charged monomers f_i was independent of the concentration, the scaling relationship between the dielectric parameters and concentration was predicted by Ito *et al.*[37] Furthermore, considering the variation of the fraction of charged monomers f_i and counter-ions distribution, Lu *et al.*[38] developed a more refined model called double layer polarization (DLP). In this refined model, the counter-ions atmosphere of a PE chain was divided into a electric double layer and a bulk layer. They illuminated the coupling of structural and counter-ions atmosphere, then concluded the dielectric function in the form of free energy storage and loss.

In previous studies the dielectric spectroscopy technique, as a non-destructive tool, has been widely used to probe the aggregation and relaxation dynamics of a representative grafted PE containing hydrophobic groups, poly(acrylic acid)-*graft*-poly(ethylene oxide)-*graft*-dodecyl (PAA-*g*-PEO-*g*-dodecyl) (Scheme 1).[39] In the present work, DRS serves as the principle technique used to investigate the conformation and counter-ions condensation effect in the PE solution. Valuable structural and electrical information on the chains and counter-ions atmosphere were obtained based on dielectric analysis *via* the DLP model. Notably, we explored the condensation of counter-ions through theoretical studies comparing the fraction of effective charges on the chains with the calculated results. A new insight to the microstructure of the chains in the different concentration ranges from the viewpoint of interactions and the effect of the condensation of counter-ions on the conformation was illuminated.

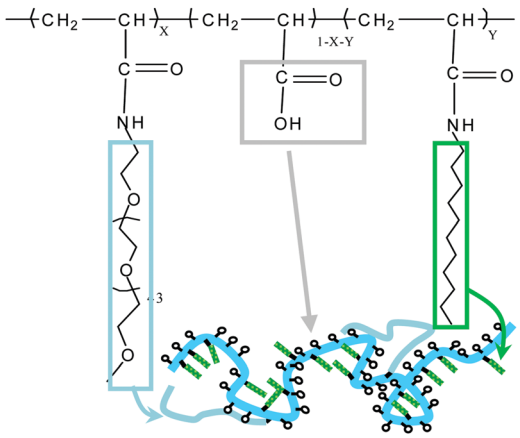

Scheme 1 The structure of the PAA-*g*-PEO-*g*-dodecyl molecules. The PEO and dodecyl are shown on the PAA main chain.

2. Model and theory

Initially, a classical DLP model for rigid PE chains was developed by Fixman *et al.*[40] In their work, a PE chain was treated as a charged cylindrical tube. The ion atmosphere around the chain was divided into an electric double layer (EDL) near the charged cylindrical tube and a diffusion layer outside the EDL. The energy of electrical repulsion between the monomers was mainly screened by the EDL in a degressive mode. Under an ac electric field, the disturbed ion atmosphere causes the slow diffusion of counter-ions along the chains and a fast diffusion of counter-ions perpendicular to the chains, respectively. Lu *et al.* elaborated the model to flexible PEs by an approximation of local stiff segments.[38] This model enables one to quantitatively describe both the conformation and ions atmosphere of flexible PE chains, as well as the interactions between them. The double-layer polarization (DLP) model of flexible PEs is illustrated in Fig. 1.

PE chains with a volume fraction of φ were dispersed in a continuous medium with a relative permittivity of ε_s (Fig. 1a). A PE chain forms a series of correlation blobs with a diameter of ξ (termed the correlation length) connected each other. Within the range of the correlation length, the electrostatic and hydrodynamic interactions stretch the chain. Thus, the PE chains adopt a random walk configuration of correlation blobs

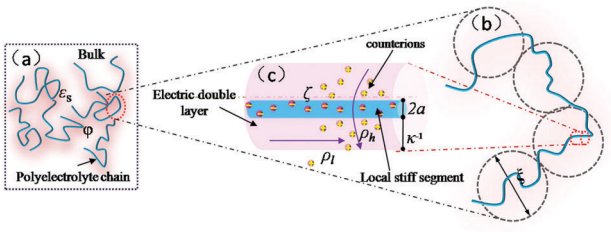

Fig. 1 (a) Schematic of the double-layer polarization (DLP) model of flexible PEs; PEs with an occupied volume fraction of φ are dispersed in a solvent with a relative dielectric constant of ε_s. (b) Chain configuration after a random walk of correlation blobs with a volume of ξ.[3] (c) Local stiff segment with a radius of a and an electric double layer (EDL) with a thickness of κ^{-1}; ζ is the surface potential of local stiff segment, ρ_l and ρ_h are the linear density of counterions fluctuating along and perpendicular to chains axes, respectively.

(Fig. 1b). A correlation blob is composed of several stiff subunits and can be regarded as a charged cylinders tube with a radius of a (Fig. 1c). The thickness of the EDL (Debye length) in the vicinity of a PE chain is κ^{-1}. On the cylinder surface ($r \to a$), the electrical potential Ψ_0 is the zeta potential ζ. While on the cylinder surface far away from the cylinder ($r \to \infty$), the electrical potential Ψ is 0. q denotes the charge of a counter-ion. When an AC electric current flows through the bulk and the double layer, the majority of the counter-ions within EDL with a charge density of ρ_h diffuse perpendicular to the chains and result to a high frequency (HF) relaxation. Other counter-ions with a charge density of ρ_l mainly diffuse along the chains with a low frequency (LF) relaxation.

When an AC electric current flows through the bulk and the double layer in series, the majority of counter-ions with charged density ρ_h within double layer are driven to diffuse perpendicular to chains, resulting to the high-frequency (HF) relaxation. While other counter-ions with charged density ρ_l mainly diffuse along chains, resulting to the low-frequency (LF) relaxation.

The complex permittivity $\varepsilon^*(\omega)$ is contributed from the counter-ions fluctuation along $\varepsilon_l{}^*(\omega)$ and perpendicular to the chains axes $\varepsilon_h{}^*(\omega)$, respectively:

$$\varepsilon^* = \varepsilon_l{}^*(\omega) + \varepsilon_h{}^*(\omega) + A\omega^{-m} - \frac{B\omega^{1-m}}{i\omega\varepsilon_0} \quad (1)$$

where ω (= $2\pi f$; f is the measured frequency) is the angular frequency, $A\omega^{-m}$ is the electrode polarization (EP) term of the permittivity data and the $B\omega^{1-m}/i\omega\varepsilon_0$ is the electrode polarization (EP) term of the dielectric loss data. A, B and m are the empirical parameters. m is related to the electrical phase angle δ (= $\pi(1-m)/2$), which can be used to characterize the electrode polarization.[41–43]

The contribution of low-frequency (LF) relaxation can be expressed as:

$$\varepsilon_l{}^*(\omega) = \frac{\Delta\varepsilon_l}{1 + \left(\frac{-i\omega\xi^2}{D_i}\right)^{\alpha}} \quad (2)$$

where ξ is the correlation length, D_i (= k_BTM_i) is the diffusivity of the counter-ions, M_i is the mobility of the counter-ions, k_BT is the thermal energy and α is the distribution coefficient of low-frequency relaxation. Based on the perturbation calculation of the PE solution, the dielectric increment can be defined as:

$$\Delta\varepsilon_l = \frac{16\pi}{9}\frac{\varepsilon_s\varphi\xi}{\nu\kappa^2}\left(\frac{G_l}{G_0}\right)^2 \quad (3)$$

where φ is the volume fraction of PE chains, G_0 (= M_iq^2/l_B) is the linear conductance of the counter-ions in the bulk. l_B is the distance at which the electrostatic interaction between two elementary charges in the medium is equal to the thermal energy k_BT. The contribution of counterion fluctuation along chains axis to linear conductance can be given as:

$$G_l = M_iq\rho_l \quad (4)$$

where the linear charged density of counter-ions that cause LF relaxation can be expressed as:

$$\rho_l = -2\pi\varepsilon_0\varepsilon_s\frac{\kappa aK_1(\kappa a)}{K_0(\kappa a)}\zeta \quad (5)$$

where ε_0 is the vacuum dielectric constant and K_α (α = 0, 1) denotes the modified Bessel function, which is usually used to describe the distribution of electric potential around a charged cylinder.

The contribution of the high-frequency (HF) relaxation can be expressed as:

$$\varepsilon_h{}^*(\omega) = \frac{\Delta\varepsilon_h}{1 + \left(\frac{-i\omega}{\omega_h}\right)^{\beta}} \quad (6)$$

where ω_h and β denote the relaxation angular frequency and the distribution coefficient of the high frequency relaxation, respectively. Eqn (7) serves as the base equation to describe the dielectric increment, $\Delta\varepsilon_h$.

$$\Delta\varepsilon_h = \frac{2}{9\pi^2}\frac{\varphi G_h{}^2\kappa}{\omega_h{}^2\varepsilon_0{}^2\varepsilon_s\nu} \quad (7)$$

The linear conductance of G_h resulting from the contribution of counter-ions fluctuation perpendicular to chain axes can be written as:

$$G_h = 2qM_i\rho_h\left(1 - \frac{1}{2\pi\eta l_BM_i}\right) \quad (8)$$

Here η is the viscosity of the solvent. The linear charged density of counter-ions, resulting in an HF relaxation of ρ_h is shown as:

$$\rho_h = \frac{\pi\varepsilon_0\varepsilon_s\zeta^2}{4k_BT}\left(\frac{\kappa aK_1(\kappa a)}{K_0(\kappa a)}\right)^2 - \frac{\pi\varepsilon_0\varepsilon_s\zeta^2(\kappa a)^2}{4k_BT} \quad (9)$$

3. Experimental and methods

3.1 Materials and preparation

3.1.1 Materials. An aqueous solution of poly(acrylic acid) (PAA) (purchased from Sigma-Aldrich with wt% = 0.35,

M_w = 2.5 × 10^5 g mol^{-1}) and 2-chloro-4,6-dimethoxy-1,3,5-triazine ethyl (CDMT) (Beijing F&F Chemical Co., Ltd) was prepared. Dodecylamine and *N*-methylmorpholine (NMM) were provided by Sinopharm Chemical Reagent Co., Ltd. Tetrahydrofuran (THF) was purchased from Beijing Chemical Works. *N*,*N*-Dimethylformamide (DMF) was purified by distillation from CaH_2 under reduced pressure. The water employed in this study was produced using a Rios-water system (Millipore Corp. America). The dialysis bag (Beijing Jingkehongda Biotechnology Co., Ltd) was pretreated with the process of successive boiling in a mixed solution of 1 : 1 ethanol/water, 0.001 M 2-[2-(bis-(carboxymethyl)-amino)ethyl(carboxymethyl)amino]acetic acid (EDTA) and 0.01 M $NaHCO_3$.

3.1.2 Preparation of samples. A solid sample of PAA-*g*-PEO-*g*-dodecyl (Scheme 1) was prepared and purified by the research group of Prof. Charles C. Han at the Chinese Academy of Sciences (Beijing, P. R. China). The coupling reagent, 4-(4,6-dimethoxy-1,3,5-triazin-2-yl)-4-methylmorpholinium chloride (DMTMM) was prepared and according to the classical reaction of an amine with a carboxylic group, PAA-*g*-PEO-*g*-dodecyl was synthesized using DMTMM. The crude product of PAA-*g*-PEO-*g*-dodecyl was dialyzed against an acidic mixed solution of water and ethanol, and then dialyzed against pure water. Finally, the solid sample was obtained after free-drying. The average molecular weight (M_w) of the PAA segments was 2.5 × 10^5 and the degree of polymerization was 3470. The weight percentage of the PEO and dodecyl side chains were 13% and 10%, respectively. Correspondingly, the molar fractions were 0.5% and 4.9%, while the average molar mass of the monomers M_{mon} was 89.337 g mol^{-1}.

The solid sample of PAA-*g*-PEO-*g*-dodecyl (170 mg) was initially dissolved in 300 μL of DMF and 10 mL of double-distilled water (the resistance was higher than 16 MΩ cm). The pH of the initial aqueous solution was controlled at around 8.0 by the slow dropwise addition of a KOH solution (0.5 mol L^{-1}). A series of aqueous solutions of PAA-*g*-PEO-*g*-dodecyl (0.0125–17 mg mL^{-1}) were prepared by adding a given volume of double-distilled water to the initial solution with a mass fraction of 17 mg mL^{-1}.

3.2 Dielectric measurements

The dielectric measurements of the aqueous solutions of PAA-*g*-PEO-*g*-dodecyl over a wide concentration range were carried out using a 4294A precision impedance analyzer (Agilent Technologies) from 40 Hz to 110 MHz. The applied alternating field was 500 mV and a measurement cell with concentrically cylindrical platinum electrodes was employed. The effective area of the electrodes was 78.5 mm^2, while the diameters of the inner and outer cylindrical electrodes were 5 mm and 10 mm, respectively. All the measurements were carried out at room temperature (30 ± 0.5 °C). Firstly, the measured raw data for the capacitance C_x and conductance G_x were corrected to minimize the errors from the residual inductance (L_r) and stray capacitance (C_r) according to Schwan's method.[41] After the correction, the capacitance C_s and conductance G_s were converted to the corresponding dielectric permittivity ε' and conductivity κ *via* the equations, $\varepsilon' = C_s/C_l$ and $\kappa = G_s\varepsilon_0/C_l$.

3.3 Determination of structural and electrical parameters

Under an applied AC electric field, the complex permittivity $\varepsilon^*(\omega)$ can be expressed as:

$$\varepsilon^*(\omega) = \varepsilon'(\omega) - j\varepsilon''(\omega) \quad (10)$$

where $\varepsilon'(\omega)$ is the real part of complex permittivity (also called permittivity) and $j = (-1)^{1/2}$, $\varepsilon''(\omega)$ is the dielectric loss, which was determined by subtracting the low-frequency limits of conductivity κ_l (termed the dc conductivity) from the total conductivity $\sigma(\omega)$ using the following equation:

$$\varepsilon''(\omega) = \frac{(\sigma(\omega) - \sigma_l)}{\omega\varepsilon_0} \quad (11)$$

The complex permittivity has been described theoretically using eqn (1)–(9) in the DLP model described in Section 2. Among these equations, lots of parameters are known or predictable, including φ, ν, ε_s, ε_0, η, l_B, T, M_i and a. Firstly, the electrode polarization of the experimental permittivity spectrums was corrected using the process described in ref. 37. Then, the experimental permittivity spectra without electrode polarization were fitted using the theoretical permittivity spectrum model, which was obtained by combining eqn (1)–(9). There have several fitting parameters including ρ_l, ρ_h, κ^{-1} and ξ. The best curve-fitting was achieved by applying the non-linear least-squares method. In this way, a set of valuable structural and electrical parameters (κ^{-1}, ξ, ρ_l and ρ_h) are determined from the fitting results. Meanwhile, the LF and HF relaxation increments ($\Delta\varepsilon_l$ and $\Delta\varepsilon_h$), which are related to ρ_l, ρ_h, κ^{-1} and ξ in eqn (3), (4) and (7), (8), were obtained, respectively. Finally, the zeta electric potentials of ζ on the surface of local stiff segments were calculated by substituting the parameters ρ_l, ρ_h and κ^{-1} based on eqn (5) and (9).

4. Results and discussion

4.1 Dielectric spectra and dielectric analysis using the DLP model

Fig. 2 shows the concentration dependence of the dielectric loss spectra of the aqueous solution of PAA-*g*-PEO-dodecyl after elimination of the EP effect. Then, the experimental dielectric loss spectra were fitted to the Cole–Cole equation.[44] The fitting result with two relaxations is displayed as the insert map in Fig. 2b. Two relaxation peaks can be easily recognized. These two peaks are related with a certain distribution from the dielectric loss spectra over the LF and HF range. Simultaneously, the black solid line in Fig. 2b was separated into two parts: the contribution from relaxation 1 in the area of light grey (LF relaxation) and the contribution from relaxation 2 in the area of dark grey (HF relaxation). Based on these observations, the aqueous solution of PAA-*g*-PEO-dodecyl possesses two relaxation processes. In addition, the concentration dependency of the dielectric loss spectra in Fig. 2a contains three groups (marked as I, II, and III) over the whole concentration

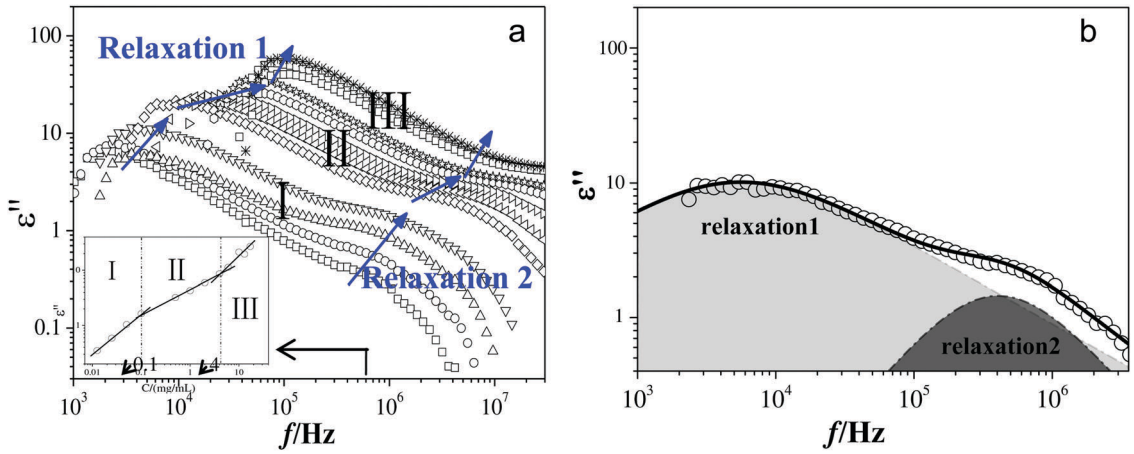

Fig. 2 (a) Dielectric loss as a function of concentration for the PAA-*g*-PEO-dodecyl aqueous solution after eliminating the effect of electrode polarization; the graph in the inset shows the concentration dependency of the dielectric loss data at a fixed frequency around 6×10^5 Hz. (b) A representative fitting result of the dielectric loss spectra for the PAA-*g*-PEO-dodecyl aqueous solution at 0.1 mg mL^{-1}.

range, which are 0.0125–0.1 mg mL^{-1}, 0.5–4 mg mL^{-1} and 4–17 mg mL^{-1}, respectively. The dielectric loss spectra of these three ranges are different from each other in their shape, as well as the concentration dependency of the position of the LF and HF relaxation peaks (blue arrows). Furthermore, two turning points around 0.1 mg mL^{-1} and 4 mg mL^{-1} are clearly shown in the result of concentration dependency of the dielectric loss around 6×10^5 in the inset of Fig. 2a. The two concentration transitions may result from some possible changes in the structural and electrical properties. These details will be discussed in the following sections.

In this work, the double layer polarization (DLP) model of flexible PE was used to analyze the permittivity spectra of the aqueous solutions of PAA-*g*-PEO-*g*-dodecyl. The analyzed method has been described in Section 3.3. Fig. 3 shows a representative fitting result for the sample at 0.05 mg mL^{-1}. It can be seen that the experimental permittivity spectra matched very well with the corresponding calculated permittivity spectra. Meanwhile, the results demonstrate the excellent performance of the DLP model in predicting the dielectric properties of PE. According to the DLP theory, there are two relaxations, which both can be observed in the graph. These two dielectric relaxation around 7 kHz and 2 MHz originate from the counter-ions fluctuating along the whole chain axes and perpendicular to the chain axes, respectively. Meanwhile, several valuable structural and electrical parameters for the samples at varying concentrations were obtained. These results are listed in Table 1. A slight rise around 10^7 Hz can be observed in Fig. 3. This might be caused by the error from the impedance analyzer and clamp, when the measurement frequency was near the upper limit. Considering this is a very small increase and a significant platform still exists in the permittivity result, such small noise does not affect the fitting results.

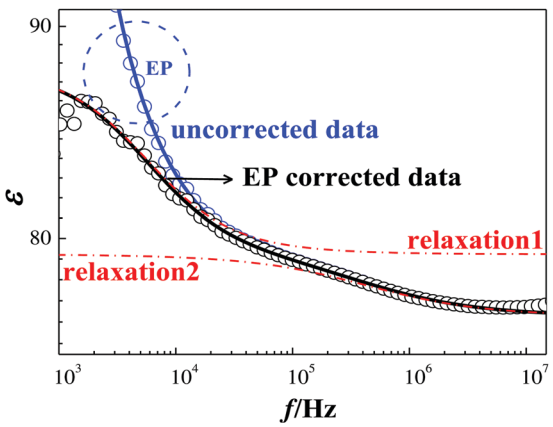

Fig. 3 A representative fitting result of the permittivity spectra of the PAA-*g*-PEO-*g*-dodecyl solution at 0.05 mg mL^{-1}. The fitting parameters include the bjerrum length l_B = 0.714 nm, the diffusivity of potassium ions $D = 0.74 \times 10^8$ nm^2 s^{-1} (ref. 45) and the measured solvent viscosity $\eta = 0.837 \times 10^{-3}$ N s^{-1} m^{-2}. The hollow circles represent the experimental permittivity data and the solid lines represent the theoretical permittivity data calculated using the DLP model. The blue and black circles (lines) are the permittivity data before and after the subtraction of the EP effect, respectively. The LF and HF relaxation are represented by the red solid lines.

4.2 Chains conformation in the different concentration regimes

Fig. 4a and b demonstrate the concentration dependency of the dielectric increment and relaxation time for the PAA-*g*-PEO-*g*-dodecyl aqueous solution, which are also listed in Table 1. From Fig. 4, there is an obvious transition over the range of 0.1–0.2 mg mL^{-1}, which is similar to the result presented in Fig. 2. In general, the PEs solution undergoes the transition in concentration range from a diluted to semi-diluted solution. Within the diluted concentration range, the PE molecules are isolated from each other and the solution properties were not influenced by the various inter-molecular interactions. When the solution concentration reaches the overlapped concentration, the PE molecules begin to interpenetrate. In this case, the properties of the PE molecules were dominated by the various inter-molecular interactions. The previous research has confirmed the presence of the crossover concentration c^* at around 0.2 mg mL^{-1} using

Table 1 Structural and electrical parameters of PAA-*g*-PEO-*g*-dodecyl in an aqueous solution at different concentrations determined using dielectric analysis (as described in Section 3.3)

c (mg mL^{-1})	$10^{19}\rho_l$ (C nm^{-1})	$10^{19}\rho_h$ (C nm^{-1})	ξ (nm)	κ^{-1} (nm)	$\Delta\varepsilon_l$	$\Delta\varepsilon_h$	τ_l (μs)	τ_h (ns)
0.0125	0.090 ± 0.003	2.20 ± 0.01	56.5 ± 0.56	40.3 ± 0.42	3.17 ± 0.19	0.200 ± 0.004	43.5 ± 0.54	225 ± 5
0.025	0.088 ± 0.003	2.15 ± 0.01	56.5 ± 0.56	39.9 ± 0.42	5.66 ± 0.26	0.257 ± 0.005	43.5 ± 0.54	203 ± 4.5
0.05	0.075 ± 0.003	2.20 ± 0.009	54.0 ± 0.54	38.6 ± 0.45	6.94 ± 0.32	1.40 ± 0.08	45.4 ± 0.44	189 ± 4.5
0.1	0.080 ± 0.003	2.05 ± 0.009	50.0 ± 0.5	38.6 ± 0.41	14.6 ± 0.57	1.79 ± 0.09	40.8 ± 0.35	167 ± 4
0.5	0.170 ± 0.005	3.75 ± 0.03	23.5 ± 0.41	15.0 ± 0.28	29.3 ± 0.87	2.41 ± 0.12	28.6 ± 0.27	99.4 ± 3
1	0.175 ± 0.005	5.00 ± 0.03	18.0 ± 0.37	12.9 ± 0.29	35.7 ± 0.89	3.00 ± 0.15	20.8 ± 0.22	67.7 ± 3
2	0.180 ± 0.005	9.25 ± 0.07	12.0 ± 0.32	10.2 ± 0.21	40.3 ± 1.36	3.16 ± 0.17	16.1 ± 0.18	43.0 ± 2.5
4	0.185 ± 0.005	11.5 ± 0.08	9.00 ± 0.28	9.56 ± 0.18	50.5 ± 1.53	3.47 ± 0.21	14.8 ± 0.16	38.8 ± 2.5
6	0.250 ± 0.008	11.8 ± 0.08	8.00 ± 0.29	7.45 ± 0.14	60.7 ± 1.39	4.50 ± 0.22	12.5 ± 0.14	37.0 ± 2
10	0.300 ± 0.007	12.5 ± 0.08	6.30 ± 0.21	5.97 ± 0.12	78.7 ± 2.04	4.85 ± 0.28	12.2 ± 0.17	34.6 ± 2
13	0.330 ± 0.009	14.8 ± 0.12	5.50 ± 0.14	5.35 ± 0.12	84.8 ± 2.51	5.21 ± 0.54	11.4 ± 0.18	32.5 ± 1.8
17	0.360 ± 0.009	13.0 ± 0.12	5.16 ± 0.17	4.82 ± 0.11	96.8 ± 2.86	5.97 ± 0.40	8.33 ± 0.10	26.5 ± 1.4

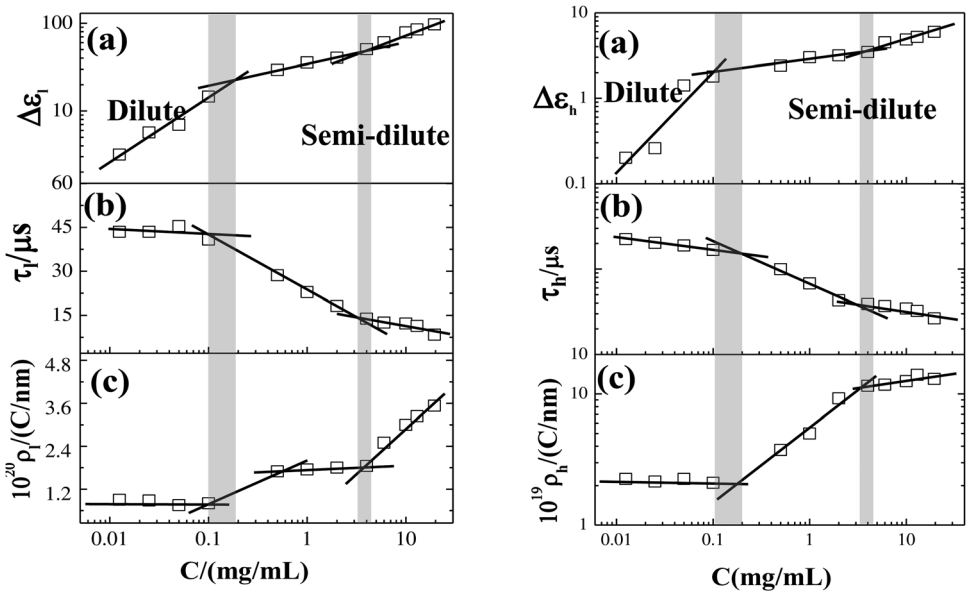

Fig. 4 Concentration dependency of the dielectric increment $\Delta\varepsilon_i$ (a), relaxation time τ_i (b) and counter-ions density ρ_i (c); i represents the LF and HF relaxation, respectively.

dielectric and light scattering measurements.[18,39] Such concentration was close to the first transition region shown in Fig. 3. Therefore, it is not difficult to conclude that the PAA-*g*-PEO-*g*-dodecyl molecules in an aqueous solution exist in the form of isolated chains below 0.1 mg mL^{-1} and as crossover chains above 0.2 mg mL^{-1}, respectively. Fig. 4c shows the plot of the linear density of counter-ions around chains as a function of the solution concentration. Remarkably, there is an abrupt increase around the crossover concentration range of 0.1–0.2 mg mL^{-1}. This result implies the overlapping electric double layers (EDL) around the chains when the solutions start to enter the semi-diluted concentration range. This provides new clues to explore the counter-ions distribution, which is hard to capture using other experimental approaches.

4.2.1 Dilute solution. In this section, the conformation of PAA-*g*-PEO-*g*-dodecyl in a diluted solution (below 0.1 mg mL^{-1}) is discussed in detail. It has been concluded that the hydrophobic interactions induced by the dodecyl side chains causes the collapse of the PEs into a globule, while the electrostatic interactions between the carboxylic groups on PAA stretches the chains. Thus, how the various interactions balance determines the conformation of the PEs worth further investigation. According to the classical theory for the chains conformation of PEs with some hydrophobic groups,[9,10] the shape of the collapsed globule will transform into a series of charged beads connected by narrow strings when the fraction of the charged monomers f_i exceeds the value of $(\tau/Nu)^{1/2}$. Here, N is the polymerization degree and τ denotes the ratio of reduced temperature shown as:

$$\tau = (\theta - T)/\theta \quad (12)$$

where θ is the theta temperature of the PE solution and the dimensionless interaction parameter u can be determined using the ratio of the Bjerrum length l_B to the bond size b:

$$u = l_B/b \quad (13)$$

In this work, the ratio of reduced temperature τ ranges from 0 to 1, while the calculated value of $(\tau/Nu)^{1/2}$ ranges from

0 to 0.0067 by substituting the Bjerrum length of ~0.7 nm and the monomer size of ~0.252 nm.[47] Meanwhile, the charged monomers fraction f_i of PAA-*g*-PEO-*g*-dodecyl at 0.0125 mg mL^{-1} was around 0.34 based on the value of the counter-ion density in Table 1. Through comparison, the fraction of charged monomers f_i was far beyond the value of $(\tau/Nu)^{1/2}$ for PAA-*g*-PEO-*g*-dodecyl in a diluted solution. According to the theory for chains conformation of PEs with some hydrophobic groups, the electrostatic repulsion on the PAA main chains was enough to resist the totally collapsed conformation due to the hydrophobic interactions originating from the dodecyl side chains. Over the dilute concentration range illustrated in Fig. 6a, the PAA-*g*-PEO-*g*-dodecyl molecules may present a necklace-like structure with a series of charged beads connected by narrow strings. Further evidence to this statement will be presented in the following section.

4.2.2 Semi-dilute solution. As mentioned above, the PAA-*g*-PEO-*g*-dodecyl molecules mainly exist in the form of overlapped chains in the semi-diluted range above 0.2 mg mL^{-1}. In this concentration range, there exists a transition point around 4 mg mL^{-1} as shown in Fig. 4a–c, which has been identified for the first time in this work. The simultaneous transition of the concentration dependences including dielectric increments, relaxation times and linear density of counter-ions shown in Fig. 4a–c indicate there is a possible change of conformation or aggregation behavior around 4 mg mL^{-1}. According to the necklace model proposed by A. V. Dobrynin *et al.*,[8,9] hydrophobic PEs possesses a necklace globule conformation. In their work, the semi-diluted range was further divided into two regions: string-controlled and bead-controlled. The logarithmic dependency of the correlation length ξ with concentration shifts around the transition concentration, which clearly implies the transformation from the string-controlled to bead-controlled region. Within the string-controlled region, a correlation blob composed of more than one hydrophobic bead connected by a series of strings is observed. The conformation is dominated by the stretched strings. Considering the contribution of the counter-ions condensation, the correlation length ξ is shown as:

$$\xi \sim b\left(uf_i^2\tau\right)^{-1/4}\left(1-\frac{cb^3}{\tau}\right)^{-1/2}\left(\frac{cb^3}{\tau}\right)^{-1/2} \quad c^* < c < c_{\mathrm{Bead}} \quad (14)$$

Similarly, within the bead-controlled region, a correlation blob composed of only one hydrophobic bead is observed. The chain conformation is mainly decided by the collapsed beads. Therefore correlation length ξ is represented as:

$$\xi \sim b\left(uf_i^2\right)^{-1/3}\left(1-\frac{cb^3}{\tau}\right)^{-2/3}\left(\frac{cb^3}{\tau}\right)^{-1/3} \quad c > c_{\mathrm{Bead}} \quad (15)$$

Such changes in the slope, which correspond to a solvophobic polyelectrolyte with pearl necklace conformation were also reported in the previously reported experimental work.[48,49] As discussed in the Section 3.3, the correlation length ξ for PAA-*g*-PEO-*g*-dodecyl in the measured concentration were obtained by dielectric analysis. Fig. 5 shows the logarithmic dependence of the correlation length ξ with concentration (Table 1). From Fig. 5, a transition point around 4 mg mL^{-1}

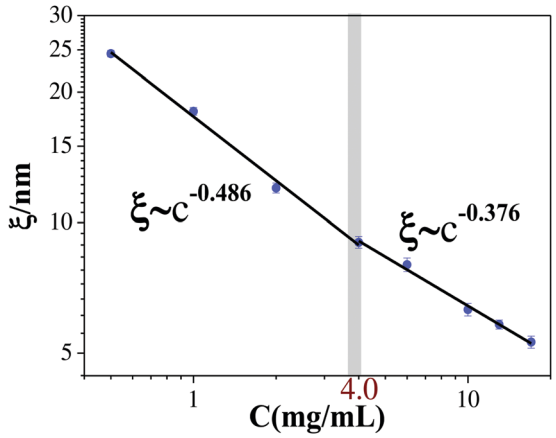

Fig. 5 The concentration dependence of the correlation length in an PAA-*g*-PEO-dodecyl aqueous solution.

was observed, which was extremely consistent with the results as shown in Fig. 4. In addition, the curve slope in Fig. 5 was −0.486 below 4 mg mL^{-1} and −0.376 above 4 mg mL^{-1}, respectively. These experimental results match very well with the theoretical value predicted from eqn (14) and (15). Such consistency strongly suggests that PAA-*g*-PEO-dodecyl in an aqueous solution adopts a necklace globule conformation with a series of beads connected by strings. 4 mg mL^{-1} is the transition concentration from the string-controlled to bead-controlled structure. The simulation results in regard the chains conformation over the different concentration ranges are illustrated in Fig. 6b and c.

4.3 Counterions condensation of PAA-*g*-PEO-*g*-dodecyl

To obtain a comprehensive understanding of the chain conformation, a further investigation into the charge properties is crucial. Firstly, the fraction of effective charged monomers of the PAA-*g*-PEO-*g*-dodecyl molecules over the entire concentration range were estimated using the counter-ions fluctuation theory. According to the theory of counter-ions fluctuation developed by Bordi *et al.*[46] there is a fluctuation of free counter-ions perpendicular to the PEs in a relatively poor solvent. Therefore, the dielectric increment ($\Delta\varepsilon_h$) and relaxation time (τ_h) follow the scaling relationship with concentration, which is represented as:

$$\Delta\varepsilon_h{}^{4/3}\tau_h{}^{-1/3} \propto c^{1/3} \quad (16)$$

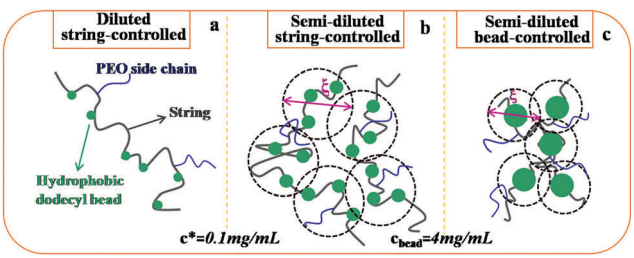

Fig. 6 Schematic of the chain conformation of PAA-*g*-PEO-*g*-dodecyl in an aqueous solution at the different concentration regime.

Fig. 7 shows the plot of $\log \Delta\varepsilon^{4/3}\tau^{-1/3}$ against $\log(c)$ based on the dielectric parameters shown in Table 1. It can be observed that there are a linear relationship between $\Delta\varepsilon^{4/3}\tau^{-1/3}$ and $\log(c)$. The slope of 0.378 was close to the theoretical value predicted by eqn (16). According to the theory of counter-ions fluctuation, the fraction of effective charged monomers f_i of PAA-*g*-PEO-*g*-dodecyl was estimated based on the dielectric increment ($\Delta\varepsilon_h$) and relaxation time (τ_h) of the leading-order HF relaxation:

$$f_i \approx \frac{\Delta\varepsilon_h}{2\pi\varepsilon_s l_B D_i \tau_h c} \quad (17)$$

In addition, the electrical nature of PAA-*g*-PEO-*g*-dodecyl in solution and the Coulombic interactions between the monomers on a chain can also be quantitatively calculated by the zeta potential of ζ, as well as the PEs and counter-ions. The calculated zeta potential and the fraction of effective charged monomers f_i are summarized in Table 2. The results demonstrate that both the ζ potential and f_i decrease when the concentration was above 0.1 mg mL^{-1}. Such phenomena are in good agreement with the concentration dependency of the ζ potential with f_i.

Theoretically, a linear relationship between the ζ potential and the negative logarithm of the counter-ion concentration in solution ($-\log c_{ion}$) was proposed by B. J. Kirby *et al.*[50]

$$\zeta = a_0 + a_1\left(-\lg\left(\frac{N}{M_w}\right)\right) + a_1(-\lg(f_i c)) \quad (18)$$

where parameters a_0 and a_1 are only decided by the solution conditions, PE composition and type of counter-ion.

The ζ potentials in Table 2 were plotted against $-\lg(f_i c)$ for the solution of PAA-*g*-PEO-*g*-dodecyl at different concentrations. As shown in Fig. 8, the linear relationship agree with the theoretical description in eqn (18). Such a linear relationship strongly suggests the applicability and feasibility of the DRS measurements in estimating the fraction of effective charged monomers f_i and ζ potential on the chains.

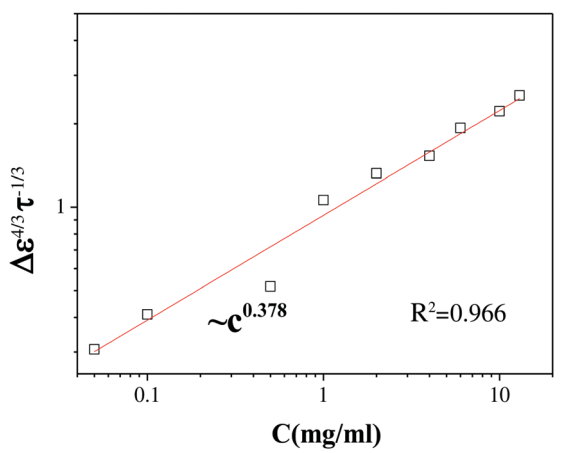

Fig. 7 Double-logarithm plot of $\Delta\varepsilon^{4/3}\tau^{-1/3}$ against c obtained using the dielectric parameter of HF relaxation shown in Table 1.

Table 2 The fraction of the effective charged monomers and zeta potential for PAA-*g*-PEO-*g*-dodecyl in an aqueous solution at different concentrations

c (mg mL^{-1})	f_i	Z (mV)	C (mg mL^{-1})	f_i	ζ (mV)
0.0125	0.34	−52.6	2	0.11	−32.7
0.025	0.26	−49.7	4	0.068	−30.0
0.05	0.37	−53.0	6	0.062	−29.3
0.1	0.32	−50.0	10	0.042	−28.1
0.5	0.15	−40.0	13	0.037	−27.7
1	0.13	−35.6	17	0.040	−27.2

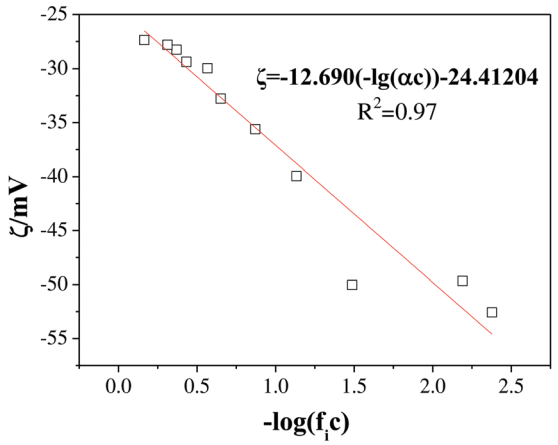

Fig. 8 Plot of ζ against $-\lg(f_i c)$ for PAA-*g*-PEO-*g*-dodecyl in an aqueous solution. The red line plots the fitting results based on eqn (18) *via* the least-squares method.

According to the Manning condensation theory, counter-ions around PE spontaneously condense onto the chains until the average distance between the charged monomers equals the Bjerrum length. In this case, the fraction of effective charges shows a logarithmical decrease with an increase in the PE concentration.[11,12,51,52]

Previous studies have reported a Manning-like counter-ions condensation for PAA.[12] In this section, the counter-ions condensation behavior of PAA-*g*-PEO-*g*-dodecyl, which is described using the results of f_i, is listed in Table 2. Moreover, the concentration dependency of f_i for PAA-*g*-PEO-*g*-dodecyl in an aqueous solution is shown in Fig. 9 (black dots and line). Over the dilute concentration range, the experimental result of f_i (the black line) is a constant instead of the general Manning condensation in which f_i logarithmically decreases as the concentration increases.[11,12,51,52] This can be explained by the low initial fraction of effective charged monomers f_{i0}, which was 0.34 at 0.0125 mg mL^{-1}. Therefore, it was not higher than the critical value of the Manning condensation, in which ξ_i was 0.36 ($\xi_i = l_B/b$). In other words, the low f_{i0} of PAA-*g*-PEO-*g*-dodecyl at 0.0125 mg mL^{-1} fails to meet the critical condition for Manning condensation to occur. Considering the low fraction of effective monomers f_i at 0.0125 mg mL^{-1}, PAA-*g*-PEO-*g*-dodecyl was a weak PE. When dissolved in water, only a portion of the free carboxylic acid groups are dissociated. On the other hand, several local hydrophobic beads on a chain with low

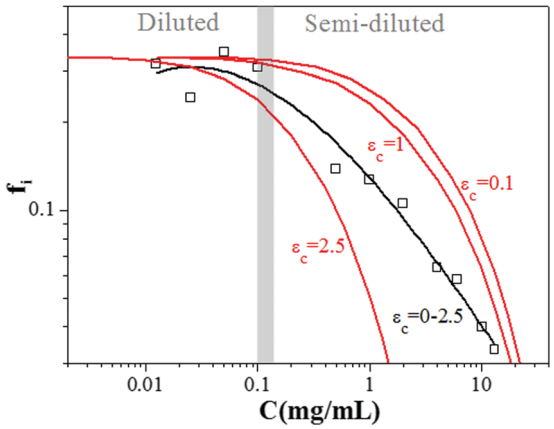

Fig. 9 Evolution of the fraction of effective charged monomers as a function of the solution concentration. The black dot (line) is the experimental data (fitted data) for PAA-*g*-PEO-*g*-dodecyl. The red line is the result given by eqn (21) with an ε_c value of 0.1, 1 and 2.5.

dielectric constant and a few water molecules further suppress the dissociation of the carboxylic groups, especially in the center of hydrophobic beads.

Over the semi-dilute concentration range above 0.2 mg mL^{-1}, as shown in Fig. 9, it was obvious that the fraction of effective charged monomers drastically decreases to lower than 0.04 above 10 mg mL^{-1}. The strong counter-ions condensation also deviated from the Manning-like condensation of PAA with an almost invariable value of f_i with concentration over the semi-dilute concentration range.[53]

In fact, an analogous counter-ions condensation has been found for poly(styrene)-*co*-styrene sulphonate, sodium salt by W. Essafi *et al.* in their experimental work.[54] Dobrynin and Rubinstein *et al.*[8,10] predicted the process of counter-ions condensation for hydrophobic PE with necklace globule conformation. A non-linear relationship between the polymer concentration c and the fraction of effective charged monomers f_i was given as:

$$c = \frac{f_{i0}\tau(f_{i0} - f_i)}{b^3\left\{f_{i0} + f_i\left[\exp\left(\frac{2f_{i0}^{1/3}\varepsilon_c}{3f_i^{1/3}}\right) - 1\right]\right\}} \quad (19)$$

where f_{i0} is the initial fraction of free counter-ion for an extremely dilute solution of hydrophobic PE. ε_c is a new parameter to characterize counter-ions energy on the surface of the necklace globule, which is expressed as:

$$\varepsilon_c = \left(\frac{l_B}{bf_{i0}}\right)^{1/3}\tau \quad (20)$$

Here, the initial fraction of free counter-ions f_{i0} was 0.34 in Section 4.3.2. ε_c ranged approximately from 0 to 2.5 by substituting f_{i0} into eqn (20). According to eqn (19), the theoretical concentration dependency was predicted, when the effective charged monomers fraction ε_c for PE were 0.1, 1 and 2.5, respectively. The corresponding results are shown in Fig. 9 (red line).

The experimental f_i–c curve of PAA-*g*-PEO-*g*-dodecyl with a ε_c value between 0 and 2.5 (black line) and theoretical f_i–c curves with different ε_c values of 0.1, 1 and 2.5 (red line) are shown in Fig. 9, respectively. On one hand, the experimental f_i–c curve ($\varepsilon_c \approx$ 0–2.5) was located between theoretical f_i–c curves with ε_c values of 0.1 and 2.5. On the other hand, the shape of the f_i–c curve was similar to the theoretical f_i–c curves, in which both curves presented avalanche-like trends. The good agreement between the experimental and theoretical f_i–c curves indicates that the counter-ions condensation behavior observed for PAA-*g*-PEO-*g*-dodecyl in an aqueous solution was more analogous to that of PE with a necklace conformation in a poor solvent. Over the semi-dilute concentration range, as the concentration increases, part of the counter-ions around the PAA-*g*-PEO-*g*-dodecyl molecules spontaneously condense into the hydrophobic beads of the necklace. The process of counter-ions condensation neutralizes some of the charges on the chains and screens the Coulombic repulsive interactions between the monomers to some degree. The PE chains further collapse and the size of the hydrophobic beads of the necklace increase due to the screening effect of the Coulombic repulsion. Subsequently, more counter-ions start to condense into hydrophobic beads with a relatively low dielectric constant. As a result of the above cyclic processes, the phenomenon of avalanche-like counter-ions condensation as shown in Fig. 9 was observed. Furthermore, as shown in Fig. 9, as the concentration increases, the rate of the decrease in f_i in the experiment (the black line) was slightly slower than f_i in theory (the red line) over the semi-dilute range. We predicted that this phenomenon probably originates from the lower loading capacity of condensed counter-ions within the hydrophobic beads formed by dodecyl side chains than those formed by the hydrophobic backbone.

4.4 The nature of conformation evolution—the role of counterions condensation and the electrostatic and hydrophobic interactions

So far, we have discussed the conformation and counter-ions condensation of PAA-*g*-PEO-*g*-dodecyl in an aqueous solution over the wide concentration range. Based on the above analysis, in this section, we aim to discuss the role of counter-ions condensation and the electrostatic and hydrophobic interactions in the chains conformation.

In the dilute solution, the conformation of a PE chain with n_A monomers separated by neighboring hydrophobic side chains containing n_B monomers (Scheme 2) has been reported from the viewpoint of the driving force by A. V. Dobrynin *et al.*[55] According to this theoretical research, the conformation of the

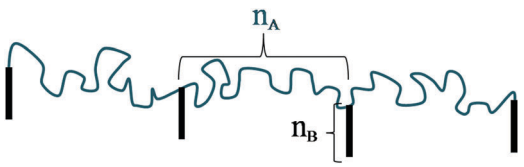

Scheme 2 Part of a polyelectrolyte (n_A = degree of polymerization) modified with hydrophobic side chains (n_B = degree of polymerization).

hydrophobic modified PE in solution was determined by the geometric ratio of the polyelectrolyte and hydrophobic side chains block as:

$$\alpha_g \approx \frac{(K_B T \varepsilon_s b n_B)^{1/3} A^{2/3}}{\tau^{1/3} e^{2/3} n_A} \quad (21)$$

and the ratio of their free energies ratio as:

$$\beta_e \approx \frac{(K_B T \varepsilon_s b n_B)^{1/3} A^{2/3} (\tau)^{4/3}}{e^{4/3} n_A} \quad (22)$$

where f_i is the fraction of effective charged monomers, e is the elementary charge, the meaning of n_A and n_B are displayed in Scheme 2. According to the theory proposed by A. V. Dobrynin *et al.*, the structure of the PEs molecules containing hydrophobic side chains in a dilute solution was determined by the geometric ratio α_g and corresponding energies ratio β_e. If α_g and β_e are both lower than 1 ($\alpha_g < 1$ and $\beta_e < 1$), the PE chains will exist with a necklace-like structure with several pendant globules (Fig. 6a) due to the strong electrostatic interactions. In this work, the α_g and β_e values of PAA-*g*-PEO-*g*-dodecyl in a dilute solution below 0.1 mg mL^{-1} were estimated to be in the range of 0.036–0.17 and 5.6×10^{-5}–0.026, respectively, which were both far smaller than 1 ($\alpha_g \ll 1$ and $\beta_e \ll 1$). Therefore, this further indicated that the PAA-*g*-PEO-*g*-dodecyl molecules in the dilute solution adopt a necklace pendant globular structure (Fig. 6a) due to the dominant contribution from the electrostatic interactions. This result greatly supports the necklace-like conformation of PAA-*g*-PEO-*g*-dodecyl.

In the semi-dilute solution, the contribution from the electrostatic interactions gradually decreases as a result of avalanche-like counter-ions condensation (Section 4.3). When the concentration was below 4 mg mL^{-1}, the electrostatic interactions remain stronger than the hydrophobic interactions, as predicted in Section 4.2. The string parts in the necklace-like conformation dominate the entire conformation (Fig. 6b). However, when the concentration was above 4 mg mL^{-1}, the contribution from the electrostatic interactions was weaker than the hydrophobic interactions. This means the entire conformation was decided by the bead part (as shown in Fig. 6c).

5. Conclusions

Over a wide concentration range, the dielectric properties of an aqueous solution of PAA grafted with hydrophobic units on part of the side chains were measured with a dielectric frequency ranging from 40 Hz to 110 MHz. After removing the electrode polarization effect, two relaxation processes around kHz and MHz were observed, respectively. A double layer polarization model (DLP) was proposed to analyze the DRS. Based on this model, various electrical and structural parameters were obtained, including the dielectric increments, relaxation time, linear density of counter-ions, correlation length, zeta potiential and Debye screening length. According to the scaling theory, a necklace-like conformation with a series of beads connected by strings was predicted. In addition to the crossover concentration around 0.1–0.2 mg mL^{-1}, there was another transition concentration around 4 mg mL^{-1}, which was identified as the transition concentration from the string-controlling to bead-controlling conformation based on the results of dielectric relaxation time, dielectric increment and linear density of the counter-ions.

Furthermore, the fraction of the effective charged monomers of PAA-*g*-PEO-*g*-dodecyl at different concentrations was estimated using the HF dielectric relaxation according to the counter-ion fluctuation theory. A theoretical linear relationship between the fraction of effective charged monomers and zeta potential were illuminated based on the experimental results. An avalanche-like counter-ions condensation was observed, which was analogous to the trend predicted by the counter-ion condensation theory of the hydrophobic polyelectrolyte with a necklace conformation. In addition, the equilibrium conformations were discussed from the aspect of the driving force. It was proven that the chains adopt a necklace-like structure with pendant globules over the dilute concentration range due to the dominant electrostatic interactions. When the concentration increased above the crossover concentration, the contribution from the electrostatic interactions gradually decreased as a result of the avalanche-like counter-ion condensation. It was concluded that the electrostatic interactions are the main driving force for the necklace-like conformation below 4 mg mL^{-1}, while the hydrophobic interaction was the main driving force for the bead-controlled necklace-like conformation above 4 mg mL^{-1}.

The present work illustrates the balance between the various interactions including electrostatic, hydrophobic and hydrophilic interactions, as well as the role of counter-ions condensation in determining the chain conformation of a polyelectrolyte with some hydrophobic groups. In addition, this work fully demonstrated the promising potential of dielectric spectroscopy technology in characterizing the physical chemistry properties of complex PEs.

Conflicts of interest

There are no conflicts to declare.

Acknowledgements

The authors gratefully thank Dr Jin-kun Hao (The Institute of Chemistry, The Chinese Academy of Science, China) for supplying the sample used in this experiment. This work was supported by the financial support from the National Natural Scientific Foundation of China (No. 21173025, 21473012, 21673002) and the Major Research Plan of NSFC (No. 21233003).

References

1 J. Kotz and S. Kosmella, Self-assembled polyelectrolyte systems, *Prog. Polym. Sci.*, 2001, **26**, 1199–1232.
2 G. Y. Bai, M. Nichifor and M. Bastos, Cationic polyelectrolytes as drug delivery vectors: calorimetric and fluorescence

study of rutin partitioning, *J. Phys. Chem. B*, 2010, **114**, 16236–16243.
3 S. M. Olveira, T. H. Silva, R. L. Reis and J. F. Mano, Hierarchical fibrillar scaffolds obtained by non-conventional layer-by-layer electrostatic self-assembly, *Adv. Healthcare Mater.*, 2013, **2**, 422–427.
4 G. H. Kirby and J. A. Lewis, Comb polymer architecture effects on the rheological property evolution of concentrated cement suspensions, *J. Am. Ceram. Soc.*, 2004, **87**, 1643–1652.
5 C. P. Vázquez, V. Dulong, C. Picart and K. Glinel, Variation of polyelectrolyte film stiffness by photo-cross-linking: a new way to control cell adhesion, *Langmuir*, 2009, **25**, 3556–3563.
6 Z. Iatridi and G. Bokias, Application of hydrophobically modified water-soluble polymers for the dispersion of hydrophobic magnetic nanoparticles in aqueous media, *Dalton Trans.*, 2014, **43**, 8633–8643.
7 P. G. De Gennes, P. Pincus, R. M. Velasco and F. J. Brochard, Remarks on polyelectrolyte conformation, *J. Phys.*, 1976, **37**, 1461–1473.
8 A. V. Dobrynin, R. H. Colby and M. Rubinstein, Scaling Theory of Polyelectrolyte Solutions, *Macromolecules*, 1995, **28**, 1859–1871.
9 A. V. Dobrynin, R. H. Colby, M. Rubinstein and S. P. Obukhov, Cascade of Transitions of Polyelectrolytes in Poor Solvents, *Macromolecules*, 1996, **29**, 2974–2979.
10 A. V. Dobrynin, R. H. Colby and M. Rubinstein, Hydrophobic Polyelectrolytes, *Macromolecules*, 1999, **32**, 915–922.
11 A. V. Dobrynin and M. Rubinstein, Counterion Condensation and Phase Separation, *Macromolecules*, 2001, **34**, 1964–1972.
12 A. Chepelianskii, F. Mohammad-Rafiee, E. Trizac and E. Raphael, On the Effective Charge of Hydrophobic Polyelectrolytes, *J. Phys. Chem. B*, 2009, **113**, 3743–3749.
13 U. Bohme and U. Scheler, Counterion condensation and effective charge of poly(styrenesulfonate), *Adv. Colloid Interface Sci.*, 2010, **158**, 63–67.
14 W. Essafi, A. Abdelli, G. Bouajila and F. Boue, Behavior of Hydrophobic Polyelectrolyte Solution in Mixed Aqueous/Organic Solvents Revealed by Neutron Scattering and Viscosimetry, *J. Phys. Chem. B*, 2012, **116**, 13525–13537.
15 Y. T. Gao, S. Wu and X. D. Ye, The effects of monovalent metal ions on the conformation of human telomere DNA using analytical ultracentrifugation, *Soft Matter*, 2016, **12**, 5959–5967.
16 L. Zeng and T. S. Zhao, An effective strategy to increase hydroxide-ion conductivity through microphase separation induced by hydrophobic-side chains, *J. Power Sources*, 2016, **303**, 354–362.
17 T. Akagi and M. Akashi, Preparation of nanoparticles by the self-organization of polymers consisting of hydrophobic and hydrophilic segments: potential applications, *Polymer*, 2007, **48**, 6729–6747.
18 J. K. Hao, C. Wu and C. C. Han, Kinetically driven intra-and interchain association of hydrophobically and hydrophilically modified poly(acrylic acid) in dilute aqueous solutions, *Macromolecules*, 2010, **43**, 9534–9540.
19 X. Wu and J. B. Wang, Self-assembly of a series of random copolymers bearing amphiphilic side chains, *J. Colloid Interface Sci.*, 2010, **349**, 560–564.
20 Z. Iatridi and G. Bokias, Application of hydrophobically modified water-soluble polymers for the dispersion of hydrophobic magnetic nanoparticles in aqueous media, *Dalton Trans.*, 2014, **43**, 8633–8643.
21 G. Y. Bai, M. Nichifor and M. Bastos, Cationic Polyelectrolytes as Drug Delivery Vectors: Calorimetric and Fluorescence Study of Rutin Partitioning, *J. Phys. Chem. B*, 2010, **114**, 16236–16243.
22 S. M. Olveira, T. H. Silva, R. L. Reis and J. F. Mano, Hierarchical fibrillar scaffolds obtained by non-conventional layer-by-layer electrostatic self-assembly, *Adv. Healthcare Mater.*, 2013, **2**, 422–427.
23 R. C. W. Liu, A. Pallier, M. Brestaz and C. Tribet, Impact of polymer microstructure on the self-assembly of amphiphilic polymers in aqueous solutions, *Macromolecules*, 2007, **40**, 4276–4286.
24 P. Kosovan, Z. Limpouchova and K. Prochazka, Conformational behavior of comb-like polyelectrolytes in selective solvent: computer simulation study, *J. Phys. Chem. B*, 2007, **111**, 8605–8611.
25 G. Cheng, B. M. Yuri, D. W. George, J. H. Feng, K. L. Hong and W. M. Jimmy, Conformational behavior of comb-like polyelectrolytes in selective solvent: computer simulation study, *Polymer*, 2007, **48**, 4108–4113.
26 A. Saheki, Y. Fukui, Y. Hoshi, J. Seki and I. Tamai, Influence of preparation method on polynucleotide conformation and pharmacological activity of lipoplex, *Int. J. Pharm.*, 2011, **406**, 117–121.
27 M. Liu, J. C. Leroux and M. A. Gauthier, Conformation–function relationships for the comb-shaped polymer pOEGMA, *Prog. Polym. Sci.*, 2015, **48**, 111–121.
28 R. P. Lorena, P. Andrew, S. Michael, B. Giuseppe, S. Ian, S. Linda and G. Mark, Conformation of Poly(methacrylic acid) Chains in Dilute Aqueous Solution, *Macromolecules*, 2008, **41**, 2203–2211.
29 J. S. Jan and V. Breedveld, Microrheological study of polyelectrolyte collapse and reexpansion in the presence of multivalent counter-ions, *Macromolecules*, 2008, **41**, 6517–6522.
30 K. Huber and U. Scheler, New experiments for the quantification of counterion condensation, *Curr. Opin. Colloid Interface Sci.*, 2012, **17**, 64–73.
31 M. Luksic, R. Buchner, B. Hribar-Lee and V. Vlachy, Dielectric Relaxation Spectroscopy of Aliphatic Ionene Bromides and Fluorides in Water: The Role of the Polyion's Charge Density and the Nature of the Counter-ions, *Macromolecules*, 2009, **42**(12), 4337–4342.
32 F. Bordi, C. Cametti and G. Paradoss, Conformation transitions in aqueous solutions of poly(L-glutamic acid): a radiowave dielectric study, *J. Phys. Chem.*, 1992, **96**, 8194–8200.
33 D. Truzzolillo, C. Cametti and S. Sennatoab, Dielectric properties of differently flexible polyions: a scaling approach, *Phys. Chem. Chem. Phys.*, 2009, **11**, 1780–1786.
34 T. Mitsumata, T. Miura, N. Takahashi and M. Kawai, Ionic state and chain conformation for aqueous solutions of

supergiant cyanobacterial polysaccharide, *Phys. Rev. E: Stat., Nonlinear, Soft Matter Phys.*, 2013, **87**, 042607.
35 Z. Chen, X. W. Li, K. S. Zhao, J. X. Xiao and L. K. Yang, Dielectric Spectroscopy Investigation on the Interaction of Poly(diallyldimethylammonium chloride) with Sodium Decyl Sulfate in Aqueous Solution, *J. Phys. Chem. B*, 2011, **115**(19), 5766–5774.
36 F. Van Der Touw and M. Mandel, Dielectric increment and dielectric dispersion of solutions containing simple charged linear macromolecules: I. Theory, *Biophys. Chem.*, 1974, **2**, 218–230.
37 K. Ito and R. Hayakawa, Crossover behavior in high-frequency dielectric relaxation of linear polyions in dilute and semidilute solutions, *Macromolecules*, 1990, **23**, 857–862.
38 C. Y. David Lu, Theory of the polyelectrolyte dielectric function, *Phys. Rev. E: Stat., Nonlinear, Soft Matter Phys.*, 2011, **84**, 041804.
39 J. L. Li and K. S. Zhao, The chain conformation and relaxation dynamics of poly(acrylic acid)-*graft*-poly(ethylene oxide)-*graft*-dodecyl in water: effect of side-chains and distribution of counter-ions, *Phys. Chem. Chem. Phys.*, 2015, **17**, 4175.
40 M. Fixman, Charged macromolecules in external fields. I. The sphere, *J. Chem. Phys.*, 1980, **72**, 5177–5186.
41 H. Schwan. Determination of biological impedances, in *Physical Techniques in Biological Research*, ed. W. L. Nastuk, Academic Press, Inc., New York, 1963.
42 K. Asami and T. Hanai, Observations and the Phenomenological Interpretation of Dielectric Relaxation due to Electrode Polarization, *Bull. Inst. Chem. Res., Kyoto Univ.*, 1993, **71**, 2.
43 F. Bordi, *et al.*, Reduction of the contribution of electrode polarization effects in the radiowave dielectric measurements of highly conductive biological cell suspensions, *Bioelectrochemistry*, 2001, **54**, 53–61.
44 K. S. Cole and R. H. Cole, Dispersion and Absorption in Dielectrics I. Alternating Current Characteristics, *Chem. Phys.*, 1941, **9**, 341.
45 H. S. Harned and R. L. Nuttall, The differential diffusion coefficient of potassium chloride in aqueous solutions, *J. Am. Chem. Soc.*, 1949, **71**, 1460–1463.
46 F. Bordi, C. Cametti, T. Gili and R. Colby, Dielectric relaxations in aqueous polyelectrolyte solutions: a scaling approach and the role of the solvent quality parameter, *Langmuir*, 2002, **18**, 6404–6409.
47 Y. Mylonas and M. Ullner, Chain conformation and intermolecular interaction of partially neutralized poly (acrylic acid) in dilute aqueous solutions, *Polymer*, 1999, **40**, 6841–6847.
48 T. A. Waigh, R. Ober and C. E. Williams, Semidilute and Concentrated Solutions of a Solvophobic Polyelectrolyte in Nonaqueous Solvents, *Macromolecules*, 2001, **34**(6), 1973–1980.
49 D. Baigl, R. Obe, D. Qu, A. Fery and C. E. Williams, Correlation length of hydrophobic polyelectrolyte solutions, *Europhys. Lett.*, 2003, **62**(4), 588–594.
50 B. J. Kirby and E. F. Hasselbrink, Zeta potential of microfluidic substrates: 1. Theory, experimental techniques, and effects on separations, *Electrophoresis*, 2004, **25**, 187–202.
51 G. S. Manning, A condensed counterion theory for polarization of polyelectrolyte solutions in high fields, *J. Chem. Phys.*, 1993, **99**, 477.
52 G. S. Manning., Limiting Laws and Counterion Condensation in Polyelectrolyte Solutions I. Colligative Properties, *J. Chem. Phys.*, 1969, **51**, 924.
53 D. T. Ruzzolillo, F. Bordi, C. Cametti and S. Sennato, Counterion condensation of differently flexible polyelectrolytes in aqueous solutions in the dilute and semidilute regime, *Phys. Rev. E*, 2009, **79**, 011804.
54 W. Essafi, F. Lafuma, D. Baigl and C. E. Williams, Anomalous counterion condensation in salt-free hydrophobic polyelectrolyte solutions: Osmotic pressure measurements, *Europhys. Lett.*, 2005, **71**, 938–944.
55 A. V. Dobrynin and M. Rubinstein, Hydrophobically modified polyelectrolytes in dilute salt-free solutions, *Macromolecules*, 2000, **33**, 8097–8105.